Zea mays-mediated fabrication and characterization of zinc oxide nanoparticles with enhanced antibacterial and antioxidant properties

M. B. Ali[a], Kh. Elmnasri[b], S. Haq[c,*], Sh. Shujaat[c], M. Hfaiedh[d], F. B. Abdallah[a], A. Hedfi[a], E. Mahmoudi[e], B. Hamouda[e], M. B. Attia[e]
[a]*Department of Biology, College of Sciences, Taif University, P.O. Box 11099, Taif 21944, Saudi Arabia*
[b]*Laboratory of bacteriological research, Institute of veterinary research of Tunisia, university of Tunis El Manar, Tunis 1006, Tunisia*
[c]*Department of Chemistry, University of Azad Jammu and Kashmir, Muzaffarabad 13100, Pakistan*
[d]*Research Unit of Active Biomolecules Valorisation, Higher Institute of Applied Biology of Medenine. University of Gabes. 4119 Mednine, Tunisia*
[e]*University of Carthage, Faculty of Sciences of Bizerte, LR01ES14 Laboratory of Environment Biomonitoring, Coastal Ecology and Ecotoxicology Unit, 7021 Zarzouna, Tunisia*

This study presents the synthesis of zinc oxide nanoparticles (ZnO-NPs) using *Zea mays* leaf extract as a natural reducing and stabilizing agent. The synthesized ZnO-NPs were comprehensively characterized using X-ray diffraction (XRD), scanning electron microscopy (SEM), energy-dispersive X-ray spectroscopy (EDX), and Fourier-transform infrared spectroscopy (FTIR). XRD analysis confirmed the crystalline nature of the NPs, while SEM revealed their morphology and size distribution. EDX confirmed the elemental composition of the synthesized ZnO-NPs, and FTIR provided insights into the functional groups involved in NPs formation. The antibacterial activity of ZnO-NPs was evaluated against a selected bacterial strain using the agar well diffusion method. The results demonstrated a zone of inhibition around the wells containing ZnO-NPs, indicating their potential antibacterial efficacy. The antioxidant activity of ZnO-NPs was assessed by their ability to scavenge ABTS (2,2'-azino-bis-(3-ethylbenzothiazoline-6-sulfonic acid)) free radicals. It was found that the scavenging activity got increased with the concentration of ZnO-NPs, indicating their potential as antioxidants.

(Received September 14, 2023; Accepted December 15, 2023)

Keywords: Zea mays, Zinc oxide, Characterization, Bio-potency

1. Introduction

Nanotechnology has evolved as a multidisciplinary field since the 21st century. Currently, it is known as the most promising technology with varied applications. Nanotechnology has become more prominent in the fields of mechanics, energy science, food, environment, pharmaceuticals, drugs, cosmetics, biomedical science, and electronics [1]. Nanomaterials are the particles with nanoscale dimensions who secure chemical steadiness owing to their large surface area to volume ratio, catalytic reactivity, optical properties, and thermal conductivity [2]. Various methods that have been used previously for the fabrication of nanoparticles include microwave assisted synthesis, autoclave synthesis, physical and chemical synthesis as well as the microorganism mediated synthesis [3]. But, all of these methods are somehow not feasible economically, owing to the utilization of some toxic compounds [4]. Currently, green synthesis has enchanted the interest of researchers as it is simple, eco-friendly, and non-pathogenic. Nanoparticles have extensive applications as antibacterial, antioxidant, and anticancer agents [5].

* Corresponding author: cii_raj@yahoo.com
https://doi.org/10.15251/DJNB.2023.184.1577

ZnO nanoparticles refer to that atypical material that portrays versatile piezoelectric, semiconducting, and pyroelectric properties along with a wide range of optical and electric applications in chemical sensors, piezoelectric devices, personal care products, paints, spin electronics, and coatings [6,7]. Zinc oxide's wide range of applications and unique properties make it an interesting entity which will serve various purposes in nanoscale materials. Owing to its direct band gap of 3.7 to 3.8nm and band gap energy of 60meV, ZnO is a material of stupendous interest as it is used for photocatalytic as well as semiconductor applications in a phenomenal way [8]. The unusual properties of ZnO transform it into a multipurpose metal oxide. In the recent past, it has been extensively used for various applications such as gas sensors, light emitting diodes, photo-catalysts, solar cells, cosmetics, and pharmaceutical industries [9,10]. Not long ago, it has been utilized as photo-catalyst and antibacterial agent [5]. Owing to the less toxic and more safe nature, these nanoparticles have been preferred in food industries for packaging and processing of food materials such as meat and vegetables. Based on the previous studies and experimental evidences, it has been reported that the ZnO-NPs are beneficial if used against bacteria as they effectively inhibit bacterial growth in minute concentration [11].

All bio-systems depend on the antioxidants for their proper functioning. In case of several diseases like cardiovascular disorders, diabetes, arthritis, and cancer, it has been observed that an oxidative stress is produced due to the overproduction of various HRRS (highly reactive radical species) [12]. Resultantly, there is an urgent need for the production of some safe, natural, more effective, and less toxic antioxidant. The abrupt increase in the antimicrobial resistance has become the global concern. Additionally, there is evidence that widespread usage of anti-inflammatory and antibacterial medications has led to the development of resistant strains that are immune to antibiotics [13]. Also, they aggravate the toxicities and have chronic effects on immune and physiological systems of humans. As a result, it is the need of the hour to search for some effective antibacterial drug that can suppress resistance without damaging the immune system [14]. The biogenically synthesized ZnO-NPs serve as effective antioxidants as they are biocompatible. They can also serve as biomedicine against various microbial ailments. They enhance the abilities of fungi and bacteria to metabolize the antibiotics, and so, play a role in improving their absorption [8].

This study focuses on the fabrication of ZnO-NPs using *Zea mays* (*maize*) extract and its physicochemical characterizations. The antioxidant and antibacterial properties of the ZnO-NPs were also tested.

2. Materials and methods

2.1. Reagents

The analytical grade chemicals and solvents used in this research work were brought from Sigma-Aldrich. The $ZnCl_2.2H_2O$ was used as precursor salt, the sodium hydroxide was used as a base for pH adjustment, and deionized water was used for the preparation of solutions. Dimethyl sulfoxide (DMSO) was used as a solvent for the suspension preparation. The agar nutrient was used to grow the bacterial culture, and ABTS was used to generate its free radicals.

2.2. Extract preparation

Zea mays leaves were collected from the local field in the village Parshali district Buner and thoroughly washed with tap water followed by deionized water. The clean leaves were then cut down into small pieces with a sterile cutter and 10 g of these cut leaves were added to an airtight jar containing 1000 mL hot water. It was left for five hours. The crude extract was then filtered to separate the leaf pieces, followed by centrifugation to eliminate uncoordinated biomolecules. The clear upper layer from the centrifuge tube was collected in a volumetric flask and stored at 4°C.

2.3. Synthesis of ZnO-NPs

The 50 mM stock solution of $ZnCl_2.2H_2O$ was prepared by dissolving 2.59 g in 1000 mL deionized water. For the synthesis of ZnO-NPs, 70 mL of the stock solution and 30 mL extract were mixed in a titration flask, and the pH was adjusted to 9 after 5 min of mixing. The reaction mixture was heated (50 °C) and stirred (250 rpm) for 40 min and aged for 6 h. The solid product obtained was collected through the centrifugation process, dried at 150°C, and stored in an airtight glass bottle.

2.4. Instrumentation

The synthesized ZnO-NPs were characterized by several physico-chemical techniques. The crystalline nature was assessed through X-ray diffraction (XRD) analysis employing the Philips X'Pert model. The crystallite size of the synthesized nanostructures was determined using the Debye-Scherrer equation. Microstructure and surface topology were examined using a scanning electron microscope (SEM), specifically the JEOL JSM-5600LV model from Tokyo, Japan. To confirm the composition of the sample, an energy-dispersive X-ray (EDX) examination was conducted. Surface functional moieties were investigated using the Nicolet 560 FTIR model, which operated within the 4000-400 cm^{-1} range.

2.5. Antibacterial activity

The antibacterial activity of ZnO-NPs against the chosen bacterial species was investigated using the agar well diffusion method. To spread bacterial cultures across agar plates, swabs were used while wells were bored with a sterile borer. The NPs suspensions were made with an ultrasonic dispersion of 0.5, 1, 2 and 4mg of these NPs in 1 mL of DMSO. At a specific volume in microliters (µL), the prepared suspension was loaded into the wells of each plate and incubated at 37°C. The activity of NPs against selected bacterial species was measured in millimeters after 24 hours (mm) [15].

2.6. Antioxidant activity

ABTS free radicals were generated by mixing ABTS solution (14 mM) with potassium persulfate solution (5mM) where the mixture was allowed to react in the dark for 16 h. The absorbance of the resulting ABTS free radical solution was checked at 734 nm. A series of reaction mixtures were prepared, each containing ABTS free radical solution and a specific concentration of ZnO-NPs (50, 100, 200, and 300 µm). The mixtures were incubated at room temperature for 30 min and the decrease in absorbance was measured using a UV-Vis spectrophotometer at 734 nm. The percentage inhibition of ABTS free radical by ZnO-NPs was calculated using equation 1, where Ac is the absorbance of ABTS radical cation solution without ZnO-NPs and As is the absorbance of ABTS radical cation solution with ZnO-NPs.

$$Antioxidant\ activity\ (\%) = \left[\frac{(A_c - A_S)}{A_c}\right] \times 100 \quad (1)$$

3. Results and discussion

3.1 XRD study

The XRD pattern of ZnO-NPs shown in Fig.1 possessed the diffraction reflections at the 2 theta position along with the hkl values 31.69 (100), 34.39 (002), 36.24 (101), 47.60 (102), 56.68 (110), 63.07 (103), 68.06 (200), which due to the constructive interference of X-rays scattered by the crystal lattice planes. These reflections represented the diffraction angles (2θ) at which the X-rays were diffracted by the crystal lattice of the ZnO-NPs. All the reflections were matched with JCPDS card 01-080-0075. The ZnO had a hexagonal wurtzite crystal structure, where the lattice was made up of alternating planes of zinc (Zn) and oxygen (O) atoms. The (hkl) values corresponded to specific crystallographic planes within the lattice.

The width of the diffraction peaks in XRD patterns was related to the size of the crystalline domains or crystallites. A broader peak indicated smaller crystallites. The Scherrer

equation (eq.2) is commonly used to estimate the average crystallite size from peak broadening: where D is the average crystallite size, K is the Scherrer constant (typically around 0.9), λ is the X-ray wavelength, β is the full width at half maximum (FWHM) of the diffraction peak and θ is the diffraction angle. The average crystallite size was 38.92 nm.

$$D = \frac{K\lambda}{\beta\cos\theta} \tag{2}$$

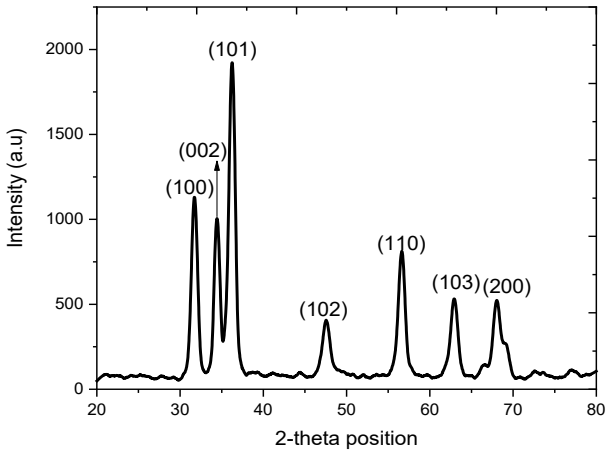

Fig. 1. XRD pattern of the ZnO-NPs.

3.2. SEM study

The SEM was used to study the surface morphology and structure of materials at high magnifications. The low and high magnification SEM images of ZnO-NPs are presented in Fig. 2, The low magnification image (a) showed that the small particles were in close contact with each other and led to the formation of different irregular shaped structures; however, the exact structures were unclear in the low magnification image. These aggregates were seen to possess almost smooth surface and were unevenly distributed, which led to the creation of different sized cavities in the sample. The presence of these cavities between the aggregated particles might be due to a lack of uniform packing during aggregation. To get more insight into the morphology of the ZnO-NPs, a high magnification image (x20,000) was acquired, which showed petals like configuration of the small particles in larger aggregates. Some of the floral/semi floral structures were seem to have stigma surrounded by petals while in other, the particles only showed the petaloid arrangement with no stigma. The number of petaloid particles were different in different aggregates and this variation in the number of petals in different flower-like structures could be attributed to different growth rates or orientations during the self-assembly process.

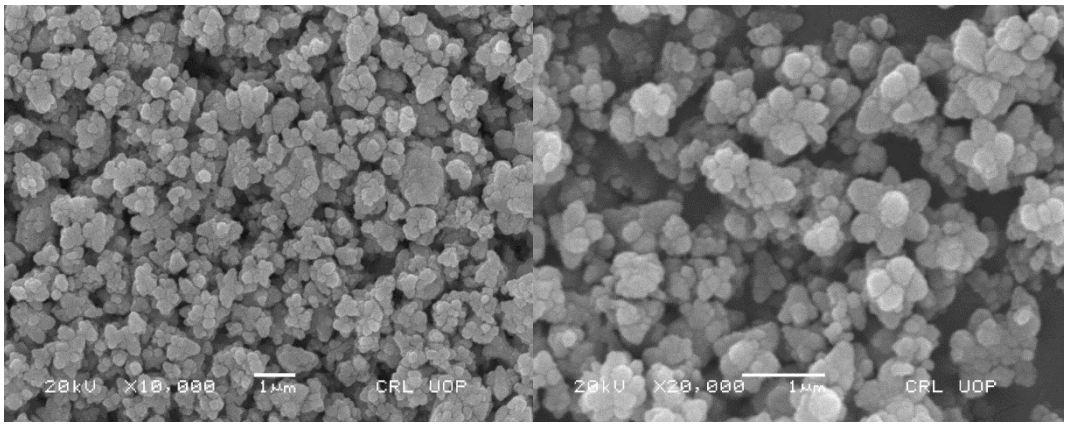

Fig. 2. Low and high magnification SEM images of the ZnO-NPs.

3.3. EDX study

The EDX was used to analyze the elemental composition of a material by detecting the characteristic X-rays emitted when the material was exposed to an electron or X-ray beam. The peaks in an EDX spectrum corresponded to the energies of these emitted X-rays and they provided information about the elements present in the sample. The EDX spectrum shown in Fig. 3, displayed peaks for zinc (Zn) that indicated the existence of different energy levels within the Zn electronic structure. The energy levels corresponded to different electronic transitions within the atom. The energy values (1 keV, 8.6 keV, and 9.5 keV) suggested that different electronic shells were involved in the X-ray emission process. The peaks at 8.6 keV and 9.5 keV likely corresponded to higher energy electronic transitions. The peak for oxygen (O) present at 0.5 keV indicated the X-ray emissions from the oxygen atoms present in the ZnO-NPs. The energy level suggested that the detected X-rays were more likely related to the K-alpha X-ray emission of oxygen. The absence of other significant peaks in the EDX spectrum could indicate that the sample primarily consisted of zinc and oxygen. The estimated weight percent along with atomic percent in parenthesis for Zn and O were 70.13(37.78) and 29.87(62.22).

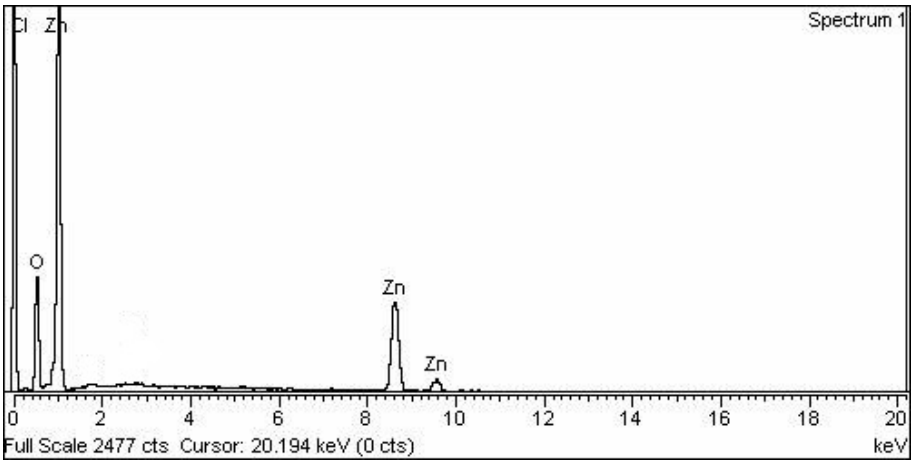

Fig. 3. EDX spectrum of the ZnO-NPs

3.4. FTIR study

The FTIR spectrum shown in Fig.4 exhibited the peaks corresponded to specific wavenumbers (cm^{-1}) at which transmission of infrared radiation occurred. The peak at 3447.61 cm^{-1} was in the region of O-H stretching vibrations. It could be indicative of hydroxyl groups or water molecules adsorbed on the surface of the NPs. The peak at 1724.74 cm^{-1} corresponding to C=O stretching vibrations was might be due to the adsorption of CO_2 on the surface of NPs. The peak 1636.93 cm^{-1} was related to the bending vibration of adsorbed water molecules or hydroxyl groups. The peak at 1359.50 cm^{-1} appeared might have been caused by the asymmetric stretching of O-Zn-O whereas the peak at 1220.79 cm^{-1} was characteristic of Zn-O-Zn stretching vibrations, indicating the bonding between zinc and oxygen in the ZnO-NPs [16]. The peak at 1089.44 cm^{-1} could be related to Zn-O stretching vibrations as well, potentially from different crystallographic directions. The peak at 615.05 cm^{-1} corresponded to Zn-O bending vibrations, providing further information about the ZnO lattice structure whereas the peak at 527.22 cm^{-1} was related to Zn-O bending vibrations, possibly from different directions. It could also be associated with lattice vibrations of ZnO.

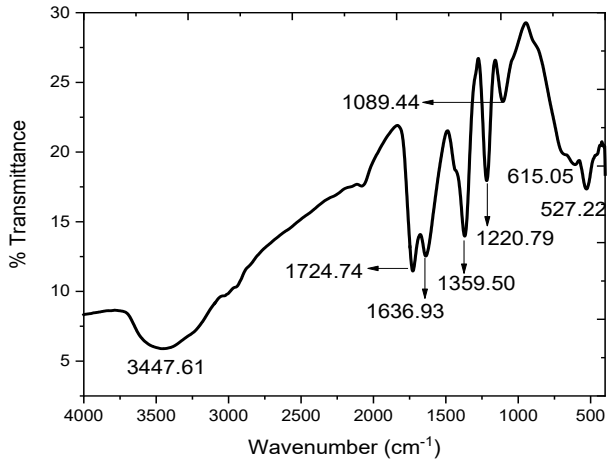

Fig. 4. FTIR spectrum of the ZnO-NPs.

3.5. Antimicrobial study

Using the agar well diffusion method, the ZnO-NPs were evaluated for their antibacterial activity against both gram positive and gram negative bacteria including *B. subtilis* and *S. aureus* as well as *E. coli* and *P. aeruginosa*, respectively. Inhibitions, measured in millimetres, were formed as a result of the activity zone as shown in Fig. 5 and table 1. According to the findings, raising the suspension concentration in wells boosted the antibacterial activity of NPs. This happened because of the smaller size and bigger surface area of ZnO-NPs, which resulted in the generation of an excessive amount of cobalt cation, which could inhibit more bacterial species [17,18].

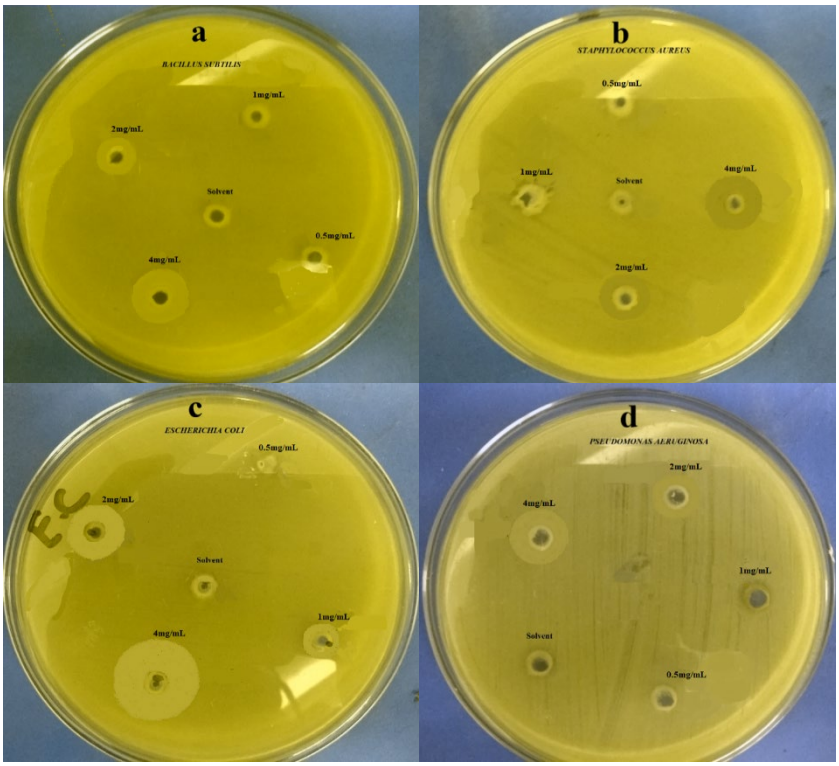

Fig. 5. Antibacterial activity of ZnO-NPs against selected bacterial strains i.e. (a= B. subtilis, b= S. aureus, c= E. coli, d= K. pneumoniae.

Table 1. Antibacterial activity of ZnO-NPs against selected bacterial strains.

Bacterial strain		Zone of inhibition in millimeter (mm)			
		0.5mg/mL	1mg/mL	2mg/mL	4mg/mL
Gram positive bacteria	*B. subtilis*	0.25 (±0.05)	0.90 (±0.05)	3.15(±0.05)	5.50(±0.05)
	S. aureus	0.78(±0.05)	1.16(±0.05)	3.80(±0.05)	6.21(±0.05)
Gram negative bacteria	*E. coli*	1.63(±0.05)	2.42(±0.05)	4.70(±0.05)	7.95(±0.05)
	P. aeruginosa	0.50(±0.05)	1.80(±0.05)	3.98(±0.05)	6.50(±0.05)

The ZnO-NPs were found to be more effective against Gram negative bacteria than Gram positive bacteria. This resulted because the cell walls of these two bacterial species had different chemical compositions. Strong peptidoglycan coating on the cell walls of gram-positive bacteria made it challenging for ZnO-NPs to enter and reduced its activity. In Gram negative bacteria, the presence of phospholipid and lipopolysaccharide had a significant surface negative charge, which interacted with ZnO-NPs and disrupted the bacterial cell [19–23].

Several methods can be used to explain the antibacterial effect of metal oxide NPs. Aqueous solutions of ZnO-NPs yield reactive species like zinc cation, super oxide radical anions, and hydroxyl radicals. Metallic oxides release metal cations, which interact with the thiol group of a vital bacterial enzyme, causing inactivation and cell death, or radicals present in aqueous ZnO-NPs interact with the negatively charged surface of the bacterial cell, disrupting vital life functions like respiration and cell replication [24–26].

3.6. Antioxidant study

The antioxidant activity of ZnO-NPs was assessed based on the percentage inhibition of ABTS free radicals where ascorbic acid was used as a standard. The results demonstrated a dose-dependent increase in antioxidant activity with increasing concentrations of ZnO-NPs (50 to 300 µg). The highest antioxidant activity was observed at the highest concentration of 300 µg/mL. The antioxidant activity of ZnO-NPs against ABTS free radicals indicated the NPs ability to neutralize these radicals, thus protecting cells and tissues from oxidative damage. In this experiment, it was observed that the antioxidant activity increased with higher doses of ZnO-NPs. The IC_{50} value of 127.65 µg/mL suggested that it took a concentration of 127.65 µg of $Zn(OH)_2$-NPs to achieve a 50% reduction in ABTS radicals, while the IC_{50} value of ascorbic acid (73.89 µg/mL) indicated its higher potency in achieving the same reduction [27].

The proposed chemical reactions to explain the neutralization of ABTS free radical cation in the presence of ZnO-NPs are given as equations 3 and 4, where the ZnO-NPs interacted with ABTS free radical cation and led to the formation of the complex (ZnO-ABTS). This complexation was probably due to the electron/hydrogen donating ability of ZnO-NPs, followed by the protonation process that led to the formation of ABTS-H. ZnO-NPs were regenerated and ready to be involved in further scavenging reactions.

$$ABTS^{\bullet+} + ZnO \rightarrow ZnO - ABTS + H^{+} \quad (3)$$

$$ZnO - ZBTS + H^{+} \rightarrow ZnO + ABTS - H \quad (4)$$

4. Conclusion

The Zea mays-mediated synthesis of ZnO-NPs yielded promising results where a highly pure product was produced that was comprehensively characterized. The process was an efficient and environmentally friendly approach for the NPs fabrication. The XRD analysis revealed the well-defined crystalline structure, while SEM images showcased the distinctive flower-like morphology of ZnO-NPs. The EDX analysis provided evidence of the elemental composition,

confirming the high purity of the obtained ZnO-NPs. FTIR spectroscopy offered insights into the functional groups present, further reinforcing their purity and successful synthesis.

The antibacterial activity demonstrated the potency of ZnO-NPs against the selected bacterial strain, with notably higher activity observed against *E. coli* compared to other bacterial strains. The ZnO-NPs exhibited antioxidant activity against ABTS free radicals, particularly at higher concentrations. This highlighted the ZnO-NPs' potential biological applications as an effective antibacterial and antioxidant agent.

Acknowledgements

The authors would like to acknowledge Deanship of Scientific Research, Taif University for funding this work.

References

[1] Abdelbaky AS, Abd El-Mageed TA, Babalghith AO, et al (2022), Antioxidants; https://doi.org/10.3390/antiox11081444

[2] Ahmad P, Khalid A, Khandaker MU, et al (2022), Materials Science in Semiconductor Processing 141:106419; https://doi.org/10.1016/j.mssp.2021.106419

[3] Aien J, Khan AA, Haq S, et al (2023), Crystals; https://doi.org/10.3390/cryst13020330

[4] Banoee M, Seif S, Nazari ZE, et al (2010), Journal of Biomedical Materials Research - Part B Applied Biomaterials 93:557-561; https://doi.org/10.1002/jbm.b.31615

[5] Bibi N, Haq S, Rehman W, et al (2020), Biointerface research in applied chemistry 10:5895–5900; https://doi.org/10.33263/BRIAC104.895900

[6] Chandra H, Patel D, Kumari P, et al (2019), Materials Science and Engineering C 102:212-220; https://doi.org/10.1016/j.msec.2019.04.035

[7] Dinesh S, Barathan S, Premkumar VK, et al (2016), Journal of Materials Science: Materials in Electronics; https://doi.org/10.1007/s10854-016-5027-y

[8] Hamid A, Haq S, Ur Rehman S, et al (2021), Chemical Papers 75:4189-4198; https://doi.org/10.1007/s11696-021-01650-7

[9] Haq S, Ali MB, Mezni A, et al (2022), Digest Journal of Nanomaterials and Biostructures 17:499-505; https://doi.org/10.15251/DJNB.2022.172.499

[10] Haq S, Rehman W, Waseem M, et al (2018a), Journal of Photochemistry & Photobiology, B: Biology 186:116-124; https://doi.org/10.1016/j.jphotobiol.2018.07.011

[11]Haq S, Rehman W, Rehman M (2020), Journal of Inorganic and Organometallic Polymers and Materials 30:1197–1205; https://doi.org/10.1007/s10904-019-01256-3

[12] Haq S, Rehman W, Waseem M (2018a), Journal of Inorganic and Organometallic Polymers and Materials 29:651–658; https://doi.org/10.1007/s10904-018-1038-x

[13] Haq S, Rehman W, Waseem M, et al (2018b), Applied Nanoscience; https://doi.org/10.1007/s13204-018-0647-6

[14] Khan S, Ansari AA, Khan AA, et al (2015 Journal of Biological Inorganic Chemistry 20:1319-1326; https://doi.org/10.1007/s00775-015-1310-2

[15] Lingaraju K, Raja Naika H, Manjunath K, et al (2016), Applied Nanoscience (Switzerland) 6:703-710; https://doi.org/10.1007/s13204-015-0487-6

[16] Mahfooz-Ur-Rehman M, Rehman W, Waseem M, et al (2019), Journal of Chemical and Engineering Data 64:2436-2444; https://doi.org/10.1021/acs.jced.8b01243

[17] Naseem T, Waseem M, Din SU, Haq S (2020), Journal of Inorganic and Organometallic Polymers and Materials; https://doi.org/10.1007/s10904-020-01529-2

[18] Patil S, Chandrasekaran R (2020), Journal of Genetic Engineering and Biotechnology; https://doi.org/10.1186/s43141-020-00081-3

[19] Raja Ahmad RA, Harun Z, Othman MHD, et al (2019), Malaysian Journal of Fundamental and Applied Sciences 15:268-273; https://doi.org/10.11113/mjfas.v15n2.1217

[20] Raza MA, Kanwal Z, Riaz S, Naseem S (2016), Advances in Civil, Environmental, and Materials Research (ACEM16) 2016:1-7.

[21] Rehman FU, Mahmood R, Ali M Ben, et al (2021), Crystal 11:1137; https://doi.org/10.3390/cryst11091137

[22] Santhoshkumar T, Rahuman AA, Jayaseelan C, et al (2014), Asian Pacific Journal of Tropical Medicine 7:968-976; https://doi.org/10.1016/S1995-7645(14)60171-1

[23] Shaban AS, Owda ME, Basuoni MM, et al (2022), Biomass Conversion and Biorefinery; https://doi.org/10.1007/s13399-022-03185-7

[24] Shah A, Tauseef I, Ali M Bin, et al (2021), Toxics 9:105-120; https://doi.org/10.3390/toxics9050105

[25] Shoukat S, Rehman W, Haq S, et al (2019), Materials Research Express 6:115052; https://doi.org/10.1088/2053-1591/ab473c

[26] Siddique S, Zain-ul-Abdin, Waseem M, et al (2021), Journal of Inorganic and Organometallic Polymers and Materials 31:1359-1372; https://doi.org/10.1007/s10904-020-01760-x

[27] Thiel J, Pakstis L, Buzby S, et al (2007), Small 3:799-803; https://doi.org/10.1002/smll.200600481